Synthesis and characterization of magnesium borate minerals of admontite and mcallisterite obtained via ultrasonic mixing of magnesium oxide and various sources of boron: a novel method

Azmi Seyhun KIPÇAK∗, **Emek MOROYDOR DERUN**, **Sabriye PİŞKİN**
Department of Chemical Engineering, Faculty of Chemical and Metallurgical Engineering,
Yıldız Technical University, İstanbul, Turkey

Abstract: Magnesium borates can be used as detergent compounds or hydrocarbon catalyzers and in the ceramics industry for superconductor material manufacture owing to their high elastic coefficient and resistance to corrosion at high temperatures. In the present study, the synthesis of magnesium borate was facilitated via a novel ultrasonic method of mixing and the identification and characterization of the material were carried out via X-Ray diffraction (XRD), Fourier transform infrared (FT-IR), and Raman spectroscopies, and the B_2O_3 content was determined through titration. The surface morphology was investigated using scanning electron microscopy (SEM). The results of the XRD analysis identified the synthesized borate compounds as admontite $[MgO(B_2O_3)_3.7(H_2O)]$, with powder diffraction file (pdf) no 01-076-0540, and mcallisterite $[Mg_2(B_6O_7(OH)_6)_2.9(H_2O)]$, with pdf no 01-070-1902. The FT-IR and Raman spectra of the obtained samples were similar, with characteristic magnesium borate bands observed in both the infrared and visible regions. The results of the B_2O_3 content analysis were in compliance with the literature. The investigation of the SEM images indicated that nanoscale minerals with a reaction efficiency ranging between 69% and 82% were obtained.

Key words: Magnesium borate, admontite, mcallisterite, ultrasonic mixing

1. Introduction

The significant boron deposits on earth are in Turkey, Russia, and the USA. The total boron reserve on Earth is 1.2 billion tons and 72.2% of this is in Turkey, followed by Russia (8.5%) and the USA (6.8%). The commercial boron reserves on earth are situated in 4 locations: the Mojave Desert in southern California, USA; the Andes Belt in South America; the Southern-Mid-Asian Orogenic Belt; and eastern Russia.[1−5]

The classification of boron minerals is handled based on their crystal structures and the complex boron (B)–oxygen (O) polyanions in these crystal structures. B may be surrounded by 3 O in the shape of a triangle or may be bound to 4 O forming a tetrahedral shape. These B–O triangles and tetrahedrons constitute the polynuclear anions sharing vertices. A proton is added to the oxygen atoms that would not be shared between the 2 boron atoms in the polyanions of hydroxy-borates and these constitute the hydroxyl groups (OH^{-1}). These polyanions combine in different forms releasing a molecule of water (H_2O) forming different boron minerals. Many synthetic borate compounds are available in addition to the many naturally occurring forms. These borates may be categorized as monoborates or polyborates. Generally, it is possible to categorize boron

∗Correspondence: skipcak@yildiz.edu.tr

minerals under 4 major titles: calcium borates, sodium borates, calcium–sodium borates, and magnesium borates.[5−7]

Magnesium borates, obtained in a relatively less refined form than the other borate minerals, are acquired through the utilization of subterrestrial mineral methods in the Liao-Dong peninsula along the North Korean border of China or through the transformation of double salts from salt water. Magnesium borates are frequently used as sources of Mg or B in place of the other refined borates or metal borates. The major areas for the use of magnesium borates are the ceramic industry, detergent compositions, superconductor material manufacture, hydrocarbon catalysis preparation, and friction-reducing additive and grease production owing to their high electric constant as well as their high resistance to corrosion at high temperatures. Additionally, they are frequently utilized in the manufacture of protective materials against neutron and gamma radiation owing to their high boron content.[5,8−12]

Despite the major part of the world's boron reserves being in Turkey, magnesium borate reserves make up a small percentage and the main forms are inderite and kurnacovite. Russia and Kazakhstan have the major magnesium borate reserve percentages.[5,8] The main objective of this study was to provide an easy and efficient approach to the production of different types of magnesium borates.

A number of different magnesium borate compounds with different compositions that are produced synthetically or acquired naturally exist and are used in different fields.[13] Zhihong and Mancheng experimented on different types of synthesis using $2MgO.2B_2O_3.MgCl_2.14H_2O$ and boric acid (H_3BO_3).[14,15] Zhu et al. produced magnesium borate hydrothermally at 240 °C using magnesium chloride ($MgCl_2$), H_3BO_3, and sodium hydroxide (NaOH)[16], whereas they obtained $MgBO_2(OH)$ by lowering the temperature to 200 °C in another study and later converted the compound to $Mg_2B_2O_5$ in a high-temperature furnace.[17] Zhihong et al. investigated the thermochemical properties of $Mg_2[B_2O_4(OH)_2].H_2O$.[18] Different types of chemical syntheses were carried out by Dou et al. at 150 °C over 6–11 h[19] and by Yılmaz at 100 °C over 8 h[20] using MgO and H_3BO_3. Several studies were carried out using borax ($Na_2B_4O_7.10H_2O$) and magnesium sulfate heptahydrate ($MgSO_4.7H_2O$) at 90 °C at 15 different reaction times, but failed to form a crystal product.[21,22] The common features of the studies that were successful in producing magnesium borate minerals were the utilization of high temperatures (>100 °C) with a hydrothermal method and extended reaction times. The failure to obtain a product with the desired crystallinity constitutes a problem regarding the investigated procedures.

Sonochemistry is an alternative method in inorganic material synthesis in recent years. The ultrasound used in sonochemistry applications facilitates different physical–chemical processes in solid, liquid, and gas media upon the cavitation bubbles losing their strength. Extremely high pressure and temperature focus may form localized short-lived hot spots in the cold fluid in response to the mechanical movement between solid and liquid interfaces during the splitting or collapsing of the cavitation bubbles.[23−25] These physical and chemical effects facilitate the formation of materials and increase the reaction rates. Ultrasound application in the synthesis of inorganic materials thus provides certain advantages over traditional methods such as low temperatures and shorter reaction times.[26]

Park et al. produced zeolite[26], Wang et al. stibnite[27], Xu et al. $BaTiO_3$,[28] and Neppolian et al. TiO_2[29] using this method.

A survey of the literature did not yield anything related to the production of magnesium borate mineral through ultrasonic mixing. However, different boron minerals were synthesized using this method. Akşener et al. produced β-barium metaborate (β-BaB_2O_4) using several boron sources such as $Na_2B_4O_7.10H_2O$,

H_3BO_3, and sodium metaborate ($NaBO_2.4H_2O$).[30] Yilmaz et al. produced sodium metaborate tetrahydrate ($NaB(OH)_4.2H_2O$) using $Na_2B_4O_7.10H_2O$ and NaOH.[31]

Derun et al. achieved the formation of different magnesium borate minerals through hydrothermal magnetic mixing of MgO and H_3BO_3 at the temperature range 80–100 °C using reaction times ranging between 30 and 240 min.[32] The present study aimed to synthesize highly efficient and highly crystalline magnesium borate minerals through the use of ultrasonic mixing methodology. The temperature of magnesium borate synthesis was lowered below 80 °C and the reaction time was reduced to less than 20 min, thus allowing energy savings. The obtained products were characterized using X-ray diffraction (XRD), Fourier-transform infrared (FT-IR) spectroscopy, Raman spectroscopy, and scanning electron microscopy (SEM) techniques.

2. Experimental Results

2.1. Results of the raw material characterization

The magnesium oxide used as the source of magnesium was determined as periclase (powder diffraction file (pdf) 01-077-2179), and the sources of boron were determined as boric acid, sassolite (pdf no 01-073-2158), and boron oxide with 2 different molecular formulae (pdf no 00-006-0297 and 01-088-2485) using XRD. The crystal systems and the lattice parameters of the raw materials are given in Table 1.

Table 1. XRD results and crystallographic data of the raw materials.

Raw material	Magnesium oxide	Boric acid	Boron oxide	
Pdf no	01-077-2179	01-073-2158	0-006-0297	01-088-2485
Mineral name	Periclase	Sassolite	Boron oxide	Boron oxide
Mineral formula	MgO	H_3BO_3	B_2O_3	B_2O
a (Å)	4.2114	7.0390	10.0550	2.8790
b (Å)	4.2114	7.0530	10.0550	2.8790
c (Å)	4.2114	6.5780	10.0550	7.0520
Crystal system	Cubic	Anorthic	Cubic	Hexagonal

2.2. XRD results of the synthesized products

The XRD results and the patterns of all products that were synthesized using ultrasonic mixing are shown in Table 2 and Figures 1a–1f. The synthesized products were determined to be admontite and mcallisterite, 2 different magnesium borate minerals.

The crystal scores (in a perfect crystal structure, where all unit cell dimensions are equal to theory, score is equal to 100) of the minerals, obtained through magnetic mixing, were determined to be higher than those obtained by Derun et al.[32] The crystallographic data of synthesized magnesium borates are given in Table 3.

The obtained product was formed in 2 distinct phases at all reaction temperatures in the MgO–H_3BO_3 (M–H) experimental setup. The highest admontite crystal score at 60 °C was achieved at reaction times of 15 or 20 min, whereas the highest mcallisterite crystal scores were obtained at a reaction time of 5 min (Figure 1a). The admontite scores were lower and the mcallisterite scores were higher at 70 °C than at 60 °C. The highest admontite crystal score was achieved after 5 min of reaction time and the highest mcallisterite score after 15 min (Figure 1b). The admontite score was observed to increase with increasing reaction times at 80 °C. The highest mcallisterite crystal score was achieved at a reaction time of 10 min (Figure 1c).
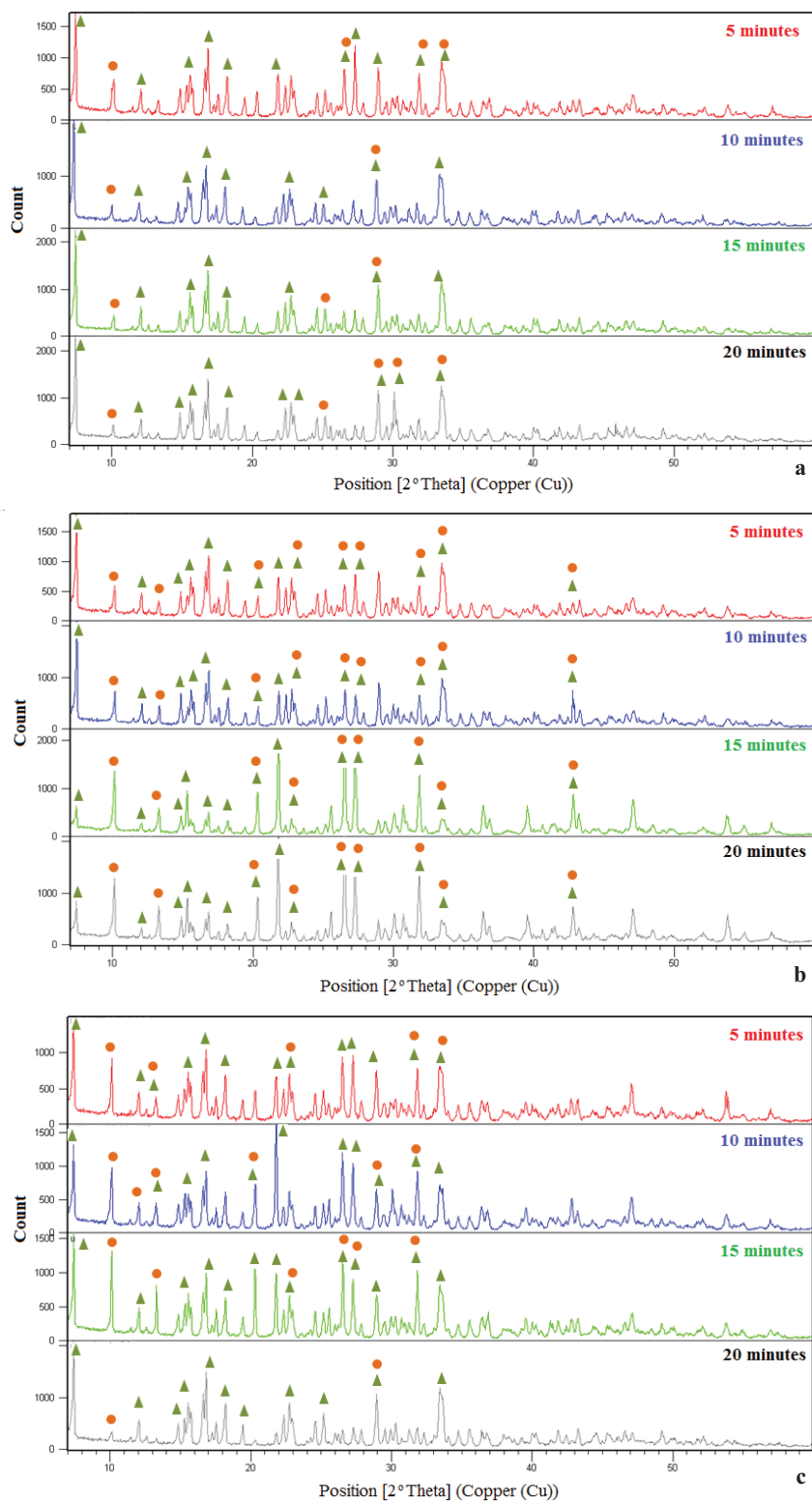
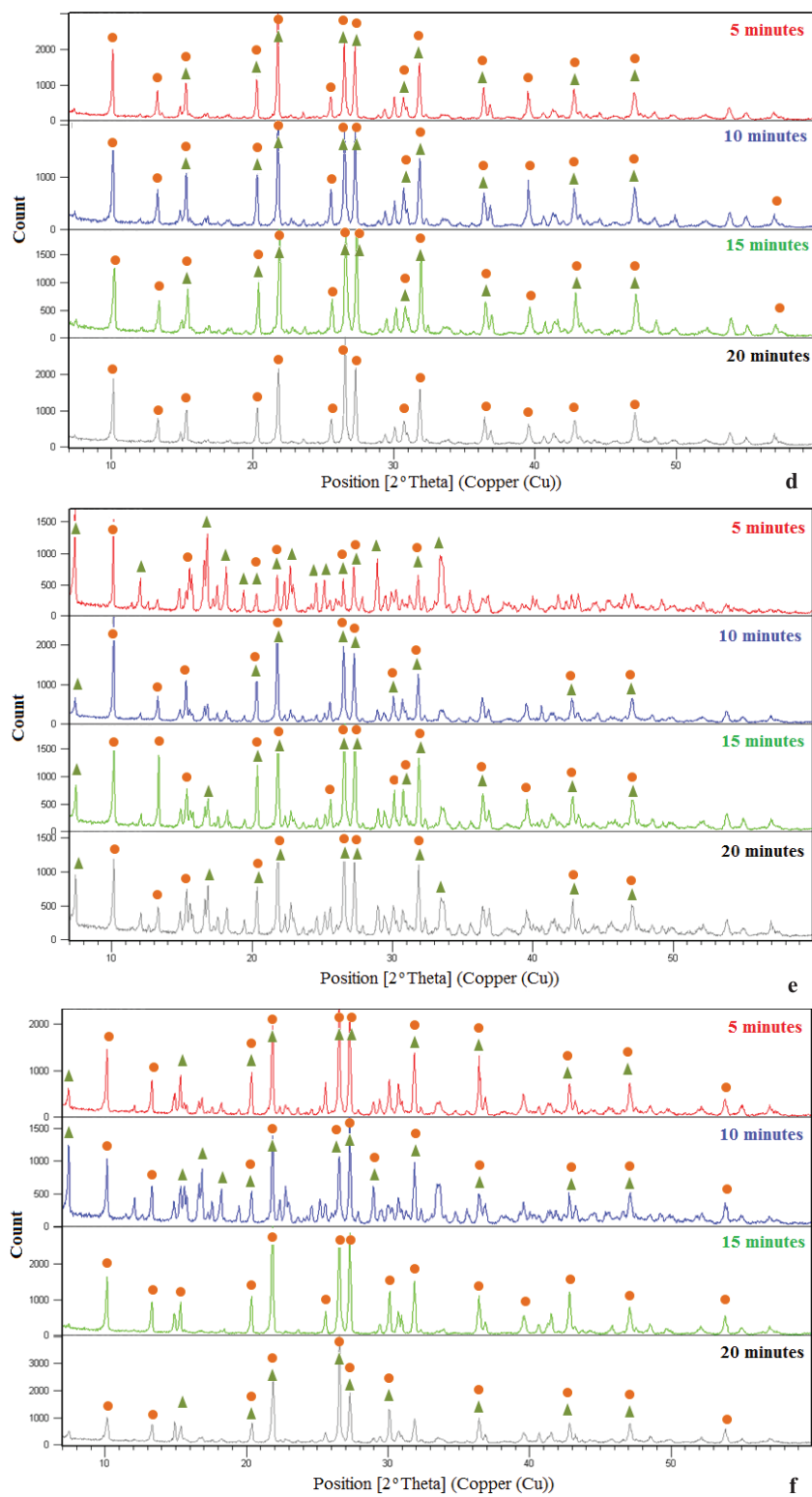**Figure 1.** XRD patterns of the products obtained from M-H at a) 60 °C. b) 70 °C. c) 80 °C

Figure 1. XRD patterns of the products obtained from M-B at d) 60 °C. e) 70 °C. f) 80 °C

Table 2. XRD results of the synthesized magnesium borate minerals.

Reaction temperature (°C)	Reaction time (min)	XRD scores of the synthesized minerals			
		M-H*		M-B*	
		▲	●	▲	●
60	5	78	78	26	88
	10	68	42	36	90
	15	80	66	36	88
	20	80	61	-	88
70	5	79	75	80	71
	10	77	74	59	84
	15	64	86	59	82
	20	68	85	71	84
80	5	76	75	55	85
	10	75	84	73	77
	15	76	80	-	86
	20	82	60	41	84

*M: MgO, H: H_3BO_3, B: B_2O_3

▲ = Admontite, pdf # = 01-076-0540, $MgO(B_2O_3)_3.7(H_2O)$

● = Mcallisterite, pdf # = 01-070-1902, $Mg_2(B_6O_7(OH)_6)_2.9(H_2O)$

Table 3. Crystallographic data of synthesized magnesium borates.

Mineral name	Admontite	Mcallisterite
Pdf	01-076-0540	01-070-1902
Chemical formula	$MgO(B_2O_3)_3.7(H_2O)$	$Mg_2(B_6O_7(OH)_6)_2.9(H_2O)$
Molecular weight (g mol^{-1})	375.27	768.56
Crystal system	Monoclinic	Rhombohedral
Space group	P21/c (No. 14)	Pr3c (No. 167)
Unit cell dimension	a = 12.6610 Å	a = 11.5490 Å
	b = 10.0910 Å	b = 11.5490 Å
	c = 11.3220 Å	c = 35.5670 Å
Z	4	6
Density (calculated)	1.83 g cm^{-3}	1.86 g cm^{-3}

Pure mcallisterite formation was observed at 60 °C after 20 min as well as at 80 °C after 15 min in the MgO–B_2O_3 (M–B) experimental setup. The products of the remaining set were bi-phasic. The admontite scores were low at 60 °C, whereas the mcallisterite scores were high. The highest admontite crystal score was achieved after allowing the reaction to proceed for 10 or 15 min and the highest mcallisterite score was achieved after 10 min (Figure 1d). The admontite scores increased at 70 °C whereas the mcallisterite scores were slightly lower than those obtained at 60 °C. The highest admontite score was achieved after 5 min. The highest mcallisterite scores were obtained after 10 or 20 min. This experimental setup was observed to produce bi-phasic products at all reaction times. The main phase was admontite after 5 min, whereas it was mcallisterite at reaction times longer than 5 min (Figure 1e). The admontite scores decreased at 80 °C and the mcallisterite scores increased. The highest admontite crystal score was achieved after 10 min. The highest mcallisterite crystal score was obtained after 15 min and that setup produced uni-phasic pure mcallisterite as the synthesized product (Figure 1f).

2.3. FT-IR and Raman spectral analysis results for the synthesized products

The structures of all synthesized magnesium borate compounds were very similar. The results were also in accordance with the results obtained in the study by Yongzhong et al. Figure 2a displays the FT-IR spectra and Figure 2b displays the Raman spectra of the magnesium borate minerals obtained from M–H at 70 °C. The band at around 1654 cm^{-1} in the FT-IR spectra corresponds to the bending of H–O–H [δ(H–O–H)]. The asymmetric stretching of the 3 coordinate boron [ν_{as}(B$_{(3)}$–O)] was observed in the range 1415–1340 cm^{-1}. The band at around 1230 cm^{-1} corresponded to δ(B–O–H) and the symmetric stretching of the 3 coordinate boron [ν_s(B$_{(3)}$–O)] was observed in the range 1083–809 cm^{-1}. δ(B$_{(3)}$–O) was observed at around 670 cm^{-1}.[33]
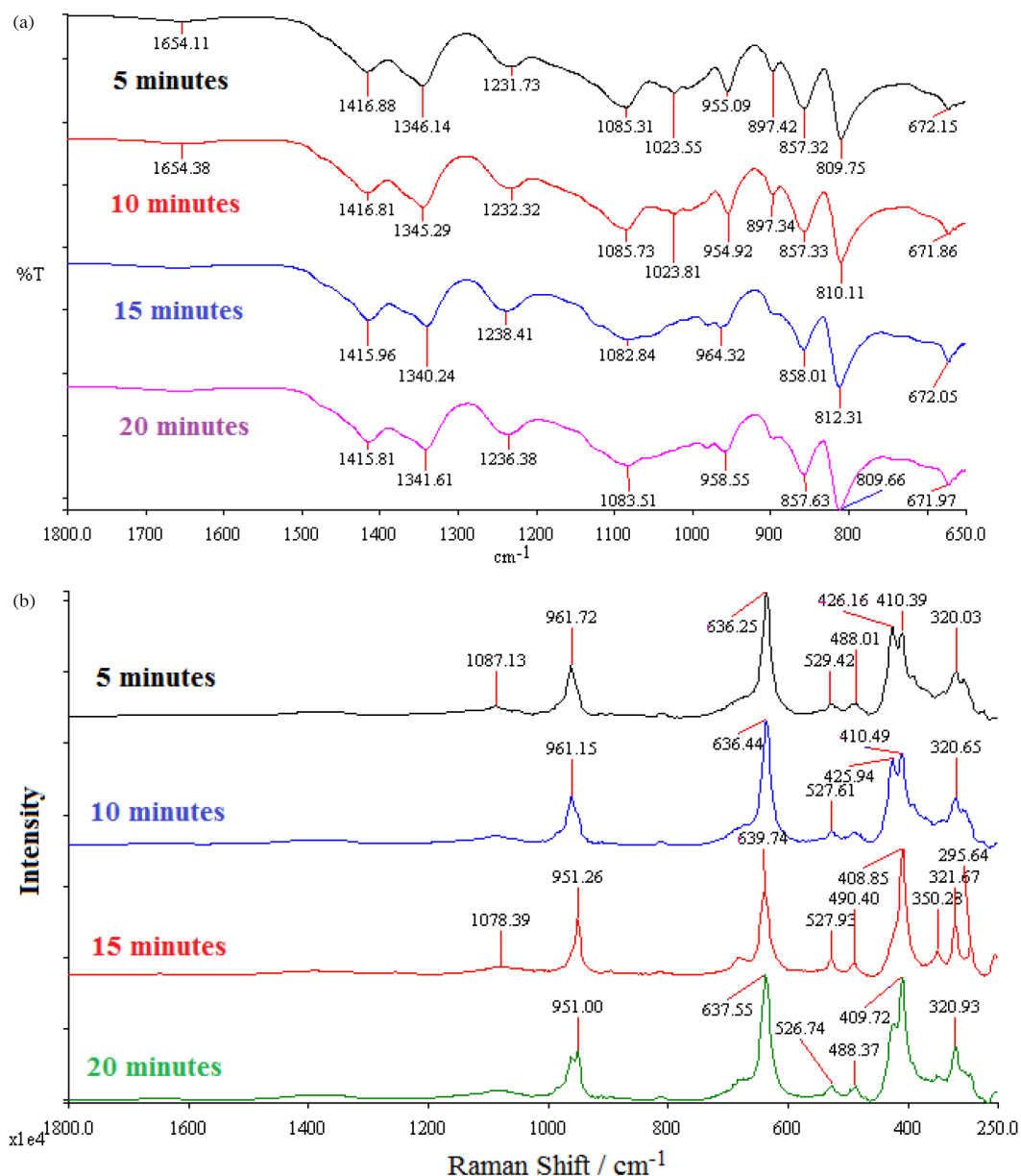

Figure 2. a) FT-IR spectra of the products obtained from M-H and 70 °C. b) Raman spectra of the products obtained from M-H and 70 °C.

The bands in the range of 1087–951 cm^{-1} in the Raman spectra were related to $\nu_{as}(\text{B}_{(4)}-\text{O})$, the bands at around 636 and 526 cm^{-1} were associated with $\nu_p[\text{B}_6\text{O}_7(\text{OH})_6]^{2-}$ / $\nu_p[\text{B}_3\text{O}_3(\text{OH})_4]^-$ and $\delta(\text{B}_{(3)}-\text{O})/\delta(\text{B}_{(4)}-\text{O})$, respectively. The bands at and below 488 cm^{-1} belonged to $\delta(\text{B}_{(4)}-\text{O})$.[33]

It is seen that the characteristic bands of magnesium borate minerals were observed and found in mutual agreement with the study by Yongzhong et al.[33]

2.4. B_2O_3 content of the synthesized products

The results of the B_2O_3 analysis of the synthesized products are displayed in Table 4. The B_2O_3 contents of the samples that were synthesized from M–H were between 40.56% and 51.60%. The B_2O_3 contents of the samples that were synthesized from M–B were between 40.93% and 53.24%.

Table 4. B_2O_3 results of the synthesized magnesium borate minerals.

Reaction time (min)	Reaction temperature (°C)	M-H B_2O_3 (%)	M-B B_2O_3 (%)
60	5	50.80 ± 1.12	45.26 ± 0.74
	10	43.64 ± 1.76	50.29 ± 0.98
	15	47.20 ± 1.48	50.20 ± 1.59
	20	45.02 ± 0.56	52.20 ± 0.74
70	5	41.28 ± 1.12	49.42 ± 1.23
	10	40.88 ± 0.56	49.25 ± 3.43
	15	40.56 ± 1.19	41.56 ± 0.98
	20	48.82 ± 0.56	51.33 ± 1.47
80	5	51.60 ± 1.12	52.02 ± 0.98
	10	49.22 ± 1.12	53.24 ± 2.70
	15	48.42 ± 1.12	40.93 ± 0.98
	20	47.23 ± 0.56	41.27 ± 0.49

2.5. Surface morphology and particle size of the synthesized products

Investigation of the SEM surface morphology of the bi-phasic magnesium borate minerals with high XRD scores, which were purely synthesized via ultrasonic mixing, revealed that the particle size of the magnesium borate minerals synthesized in the present study via ultrasonic mixing was smaller than those synthesized in the study by Derun et al.[32] via magnetic mixing, which were found between 2.52 and 12.30 μm. Generally the particle sizes were given in solid-state synthesis methods; for example, Zhu et al. synthesized $\text{MgBO}_2(\text{OH})$[16] nanowires with a length of 0.5–0.9 μm and a diameter of 20–70 nm, and synthesized $\text{Mg}_2\text{B}_2\text{O}_5$[17] with a length of 0.47–1.3 μm and a diameter of 55–160 nm. Elssfah et al. also synthesized $\text{Mg}_2\text{B}_2\text{O}_5$ with a diameter between 70 and 120 nm.[34] $\text{Mg}_3\text{B}_2\text{O}_6$-type magnesium borate was synthesized by Zhang et al.[35] $\text{Al}_{18}\text{B}_9\text{O}_{33}$ and MgB_4O_7 were synthesized by Ma et al. with a typical width of 10–100 nm.[36]

SEM analyses were conducted on samples with simultaneously high admontite and mcallisterite crystal scores and on samples that were purely mcallisterite. The obtained magnesium borate crystals were layered, sharp edged, and agglomerated as well as locally porous. The size distribution (though varying due to the agglomerated structure) of the magnesium borate minerals that were synthesized at 60 °C with a reaction time of 15 min ranged between 500.31 nm and 7.34 μm (Figure 3a), while those synthesized at 70 °C with a reaction time of 20 min ranged between 488.94 nm and 4.19 μm (Figure 3b) and those synthesized at 80 °C with a

reaction time of 10 min ranged between 654.91 nm and 2.70 μm (Figure 3c) for the M–H set. The maximum particle size was observed to decrease with increasing reaction temperature.
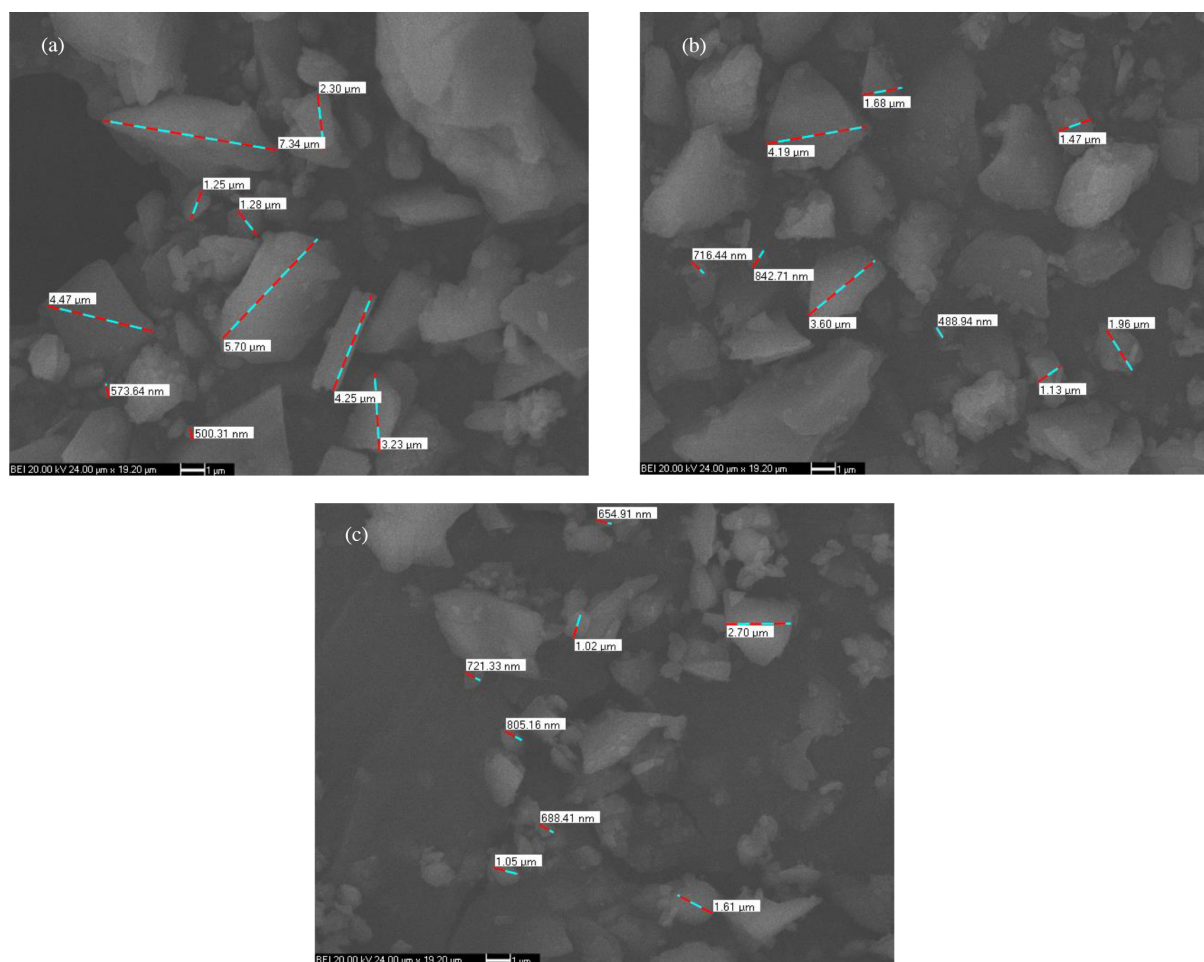

Figure 3. SEM images (5000x) of the products obtained from M-H a) 60 °C with a reaction time of 15 min. b) 70 °C with a reaction time of 20 min. c) 80 °C with a reaction time of 10 min.

The size distribution of the magnesium borate minerals synthesized at 60 °C with a reaction time of 20 min ranged between 427.57 nm and 5.00 μm (Figure 4a), those synthesized at 70 °C with a reaction time of 20 min ranged between 419.26 nm and 3.63 μm (Figure 4b), and those synthesized at 80 °C with a reaction time of 15 min ranged between 414.20 nm and 5.81 μm (Figure 4c) for the M–B set. The minimum particle size was observed to decrease with increasing reaction temperature.

2.6. Yield calculation of the synthesized product

The yield calculation of the bi-phasic samples was carried out based on the phase with the highest molecular weight. Reaction yield increased with increasing reaction temperature and time for both sets. The yield was calculated as 78%–82% for the M–H set and as 69%–74% for the M–B set. The yield of the pure mcallisterite minerals that were synthesized at 60 °C with a reaction time of 20 min was 70.52 ± 0.85% and the yield of minerals that were synthesized at 80 °C with a reaction time of 15 min was 73.82 ± 0.64%.
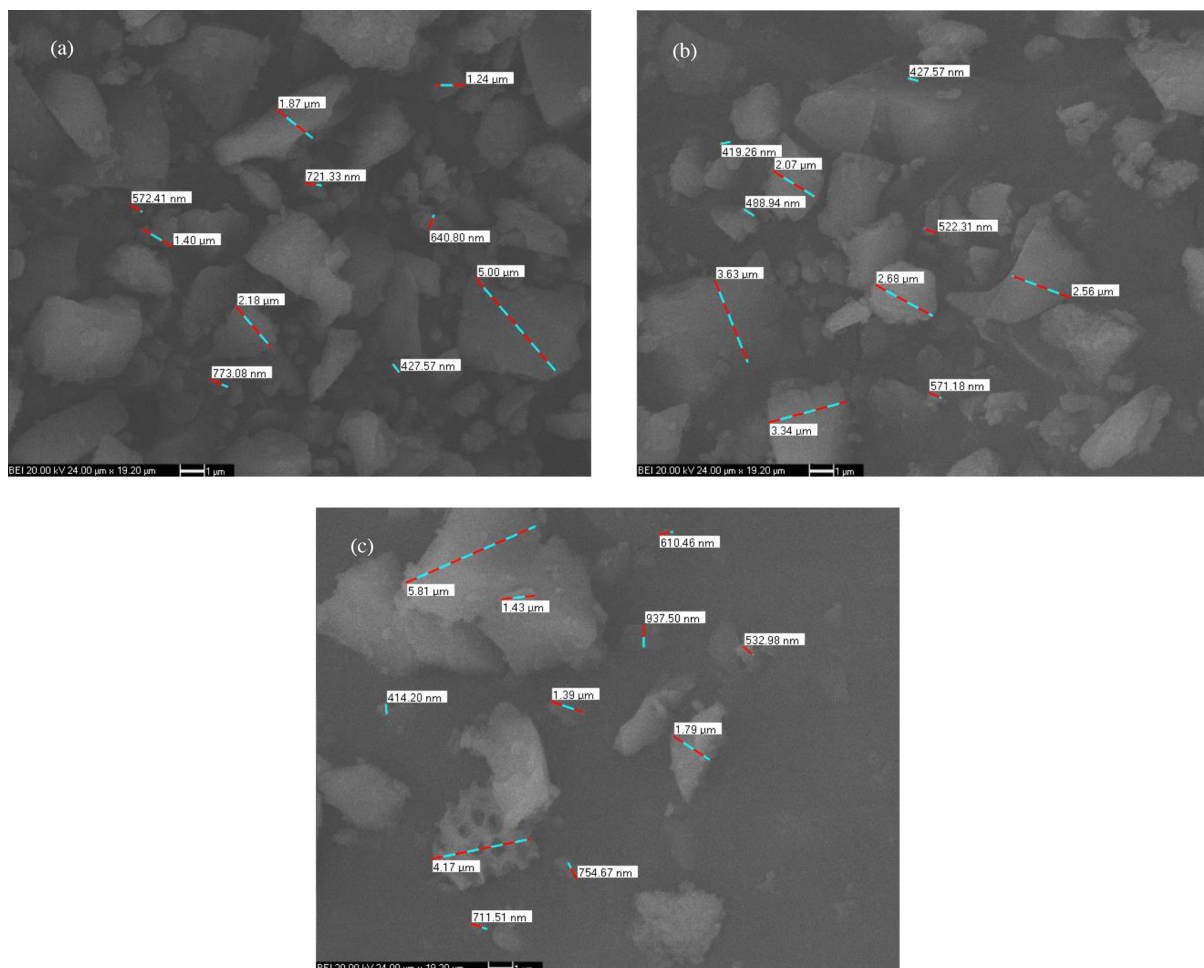
Figure 4. SEM images (5000x) of the products obtained from M-B a) 60 °C with a reaction time of 20 min. b) 70 °C with a reaction time of 20 min. c) 80 °C with a reaction time of 15 min.

3. Experimental

3.1. Preparation and characterization of the raw materials

Magnesium oxide was obtained from VWR International (Batch: 11A060010) at 99.3% purity, while boric acid (H_3BO_3) and boron oxide (B_2O_3) were obtained from Eti Mine Bandırma Boron Works at 99.0% purity. The MgO was not pretreated. The H_3BO_3 and B_2O_3 were processed by crushing, grinding through an agate mortar (Retsch RM200), and sieving through a Fritsch shaker sieve to reduce particle size to below 75 μm. The prepared samples were identified in a Philips PANanalytical X'Pert PRO XRD (Step: 0.030°, Time for step: 0.50 s, Scan speed: 0.060 °C/s, Range: 7°–90°) using the parameter values of 45 kV and 40 mA through the X-rays obtained in the Cu–Kα tube.

3.2. Magnesium borate synthesis via ultrasonic mixing

Preliminary analyses were carried out using different mole ratios of Mg:B (1:2, 1:4, 1:6, and 1:8). Increasing amounts of MgO were detected at Mg:B ratios of 1:2 and 1:4, whereas an increasing amount of H_3BO_3 was

identified at a Mg:B ratio of 1:8. The use of a mole Mg:B ratio of 1:6 throughout the analysis was adopted as a result of the preliminary experiments.

The pure water used in the experiments was obtained from a Human Power I+ water treatment system and had a conductivity value of 18.3 mΩ cm. The reaction temperatures were determined as 60, 70, and 80 °C, whereas the reaction time parameters were determined as 5, 10, 15, and 20 min as a result of other preliminary experiments. The mixer used in the experiments was a Bandelin Sonoplus HD 2070 with an ultrasonic probe having 90% power and 80% cycle. The experiments were carried out in a closed container and the reaction temperature was maintained constant via a temperature control unit. The product was separated from unreacted MgO at the end of the allowed reaction time by filtering the product into a beaker under vacuum. The excess water in the beaker was evaporated and the solution was kept in an incubator maintained at 40 °C until the magnesium borate minerals crystallized. The incubator-dried samples were washed thoroughly with 96%
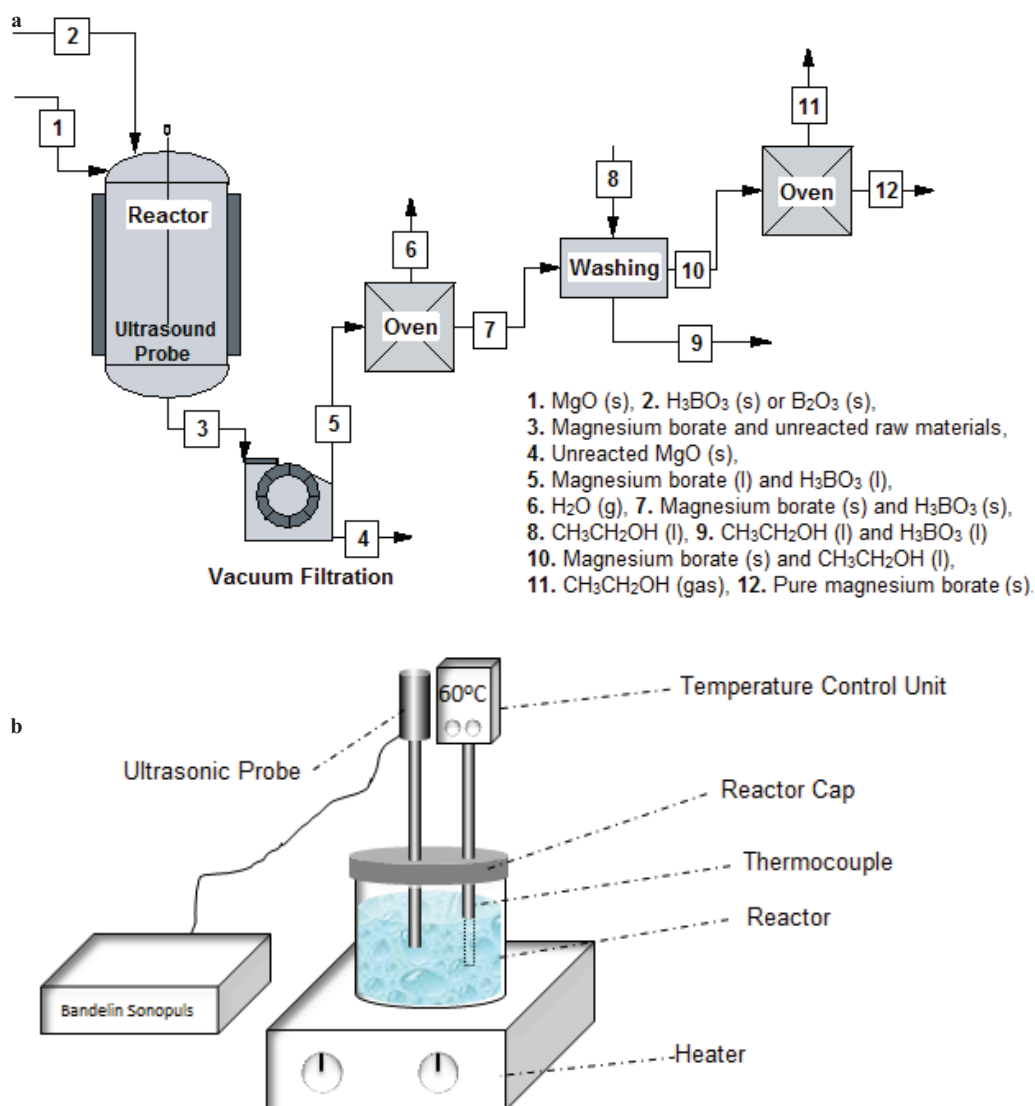

1. MgO (s), 2. H₃BO₃ (s) or B₂O₃ (s),
3. Magnesium borate and unreacted raw materials,
4. Unreacted MgO (s),
5. Magnesium borate (l) and H₃BO₃ (l),
6. H₂O (g), 7. Magnesium borate (s) and H₃BO₃ (s),
8. CH₃CH₂OH (l), 9. CH₃CH₂OH (l) and H₃BO₃ (l)
10. Magnesium borate (s) and CH₃CH₂OH (l),
11. CH₃CH₂OH (gas), 12. Pure magnesium borate (s).

Figure 5. a) Experimental method. b) The reaction scheme.

ethyl alcohol (CH_3CH_2OH) and thus separated from the unreacted H_3BO_3. The magnesium borate minerals remaining on the filter paper were removed from CH_3CH_2OH by leaving the minerals in the incubator at $40\,^\circ C$. The experimental method and the reaction scheme are shown in Figures 5a and 5b, respectively.

3.3. Product characterization studies

The samples that were ready for analysis were processed through XRD, FT-IR, and Raman spectral analyses in the given order. The XRD analyses were carried out using the parameters indicated in Section 3.1, except "Range" is selected between 7° and 60° because the characteristic peaks of magnesium borates were seen at that range.[31] The spectrum range was selected as 1800–650 cm^{-1} in the FT-IR analyses and as 1800–250 cm^{-1} in the Raman spectral analyses. No band above 1800 cm^{-1} was observed in either of the spectral analyses and the characteristic bands of borate compounds were reported to be observed in the range of 500–1500 cm^{-1}.[33] The surface morphologies of the synthesized magnesium borate minerals and their particle size analyses were carried out using CamScan Apollo 300 Field-Emission SEM at 20 kV. The selected detector was back scattering electron (BEI) and the scale of magnification was 5000.

Proven total world boron reserves on the basis of B_2O_3 content are 369 million tons. Furthermore, probable and possible reserves are 807 million tons, making a total of 1176 million tons. Turkey's share is 72.20% with total reserves of 851 million tons on the basis of B_2O_3 content.[5] Since commercial boron minerals were identified by B_2O_3 contents, the B_2O_3 content was determined using the method reported by Derun et al.[32]

Yield analysis was also carried out using the method reported by Derun et al. Magnesium oxide was identified as the key component in this method, the experimental runs were carried out in triplicate, and the average yields and the standard deviations were calculated. The number of moles of product at the final stage, N_D, was divided by the number of consumed moles of the key reactant A to calculate the overall yield, Y_D (Eq. (1)). The number of A that was consumed was calculated using the initial (N_{A0}) and the final (N_A) moles of the reactant. The equation then becomes as follows for a batch system:[32,37]

$$Y_D = \frac{N_D}{N_{A0} - N_A} \tag{1}$$

4. Conclusions

The present study aimed to synthesize magnesium borates via a novel method of ultrasonic mixing at lower reaction temperatures in shorter reaction times. Derun et al.[32] synthesized magnesium borate at a reaction temperature of 80–100 °C in a reaction time of 30–240 min, whereas the proposed method reduced the reaction temperature to 60 °C and the reaction time to 5 min. Furthermore, the biggest advantage of the method was the obtaining of pure magnesium borate minerals. The yield of the obtained product ranged between 69% and 82% and the XRD crystal scores were as high as 90. The highest crystal score in the study by Derun et al.[32] was 61. The particle size of the synthesized particles was determined to be as low as 400 nm via the ultrasonic method, whereas the particle size was greater than 2 μm in the study by Derun et al.[32] In conclusion, the present method facilitated the synthesis of small particle size minerals of magnesium borate at lower reaction temperatures with reduced reaction times.

References

1. Davies, T. W.; Çolak, S.; Hooper, R. M. *Powder Technol.* **1991**, *65*, 433–440.

2. Eymir, C.; Okur, H. *Thermochim. Acta* **2005**, *428*, 125–129.

3. Erdoğan, Y.; Zeybek, A.; Şahin, A.; Demirbaş, A. *Thermochim. Acta* **1999**, *326*, 99–103.

4. Tunç, M.; Erşahan, H.; Yapıcı, S.; Çolak, S. *J. Therm. Anal. Calorim.* **1997**, *48*, 403–411.

5. TR Prime Ministry SPO. Chemical Industry Private Expertise Commission. Boron Operations Group Report: Ninth development plan (2007-2013) (2006) (in Turkish).

6. Çeçen, D. *Madencilik, Maden Mühendisleri Odası Yayını* **1969**, *8*, 10–18 (in Turkish).

7. Jun, L.; Shiyang, G.; Shuping, X.; Bing, L., Rongzu, H. *J. Chem. Thermodyn.* **1997**, *29*, 491–497.

8. Kıpçak, A. S. MS, Institute of Science and Engineering, Yildiz Technical University, TR, 2009 (in Turkish).

9. Derun, E. M.; Kipcak, A. S. *J. Radioanal. Nucl. Ch.* **2012**, *292*, 871–878.

10. Kipcak, A. S.; Senberber, F. T.; Baysoy, D. Y.; Derun, E. M.; Piskin, S. In *Characterization of the Synthesized Admontite Mineral and Investigation of its Neutron Permeability*, Proceedings of the 3rd International Conference on Nuclear & Renewable Energy Resources (Nurer 2012), İstanbul, Turkey, 20–23 May 2012, *paper ID: 72*, pp. 1–6.

11. Kipcak, A. S.; Baysoy, D. Y.; Derun, E. M.; Piskin, S. *Research Bulletin of the Australian Institute of High Energetic Materials* **2011**, *November*, 38–46.

12. Kipcak, A. S.; Baysoy, D. Y.; Derun, E. M.; Piskin, S. *Research Bulletin of the Australian Institute of High Energetic Materials* **2011**, *November*, 28–38.

13. Obut, A.; Girgin, I. In *Magnezyum Boratların Sentezlenmesi ve Tanımlanması*, Proceedings of the 2nd International Boron Symposium, Eskişehir, Turkey, 2004, pp. 133–138 (in Turkish).

14. Zhihong, L.; Mancheng, H. *Thermochim. Acta* **2003**, *403*, 181–184.

15. Zhihong, L.; Mancheng, H. *Thermochim. Acta* **2004**, *411*, 27–29.

16. Zhu, W.; Zhang, X.; Xiang, L.; Zhu, S. *Nanoscale Res. Lett.* **2009**, *4*, 724–731.

17. Zhu, W.; Li, G.; Zhang, Q.; Xiang, L., Zhu, S. *Powder Technol.* **2010**, *203*, 265–271.

18. Zhihong, L.; Mancheng, H.; Shiyang, G. *J. Therm. Anal. Calorim.* **2004**, *75*, 73–78.

19. Dou, L.; Zhong, J.; Wang, H. *Phys. Scripta* **2010**, *T139*: 014010.

20. Yılmaz, A. MS, Institute of Pure and Applied Sciences, Marmara University, TR, 2005 (in Turkish).

21. Koruk, M. MS, Institute of Graduate Studies in Science, Hacettepe University, TR, 2006 (in Turkish).

22. Koruk, M.; Girgin, I. *J. Non-Cryst. Solids* **2009**, *355*, 965–969.

23. Luche, J. L. *Synthetic Organic Sonochemistry*, Plenum Press: New York, NY, USA, 1998.

24. Suslick, K. S. In *Sonochemistry Kirk-Othmer Encyclopedia of Chemical Technology* 4th edn., J. Wiley & Sons: New York, NY, USA, 1998, pp. 517–541.

25. Thompson, L. H.; Doraiswamy, L. K. *Sonochemistry: Science and Engineering Industrial and Engineering Chemistry Research* **1999**, *38*, 1215–1249.

26. Park, J.; Kim, B. C.; Park, A. S.; Park, H. C. *J. Mater. Sci. Letters* **2001**, *20*, 531–533.

27. Wang, H., Lu, Y. N.; Zhu, J. J.; Chen, H. Y. *Inorg. Chem.* **2003**, *42*, 6404–6411.

28. Xu, M.; Lu, Y.; Liu, Y.; Shi, S.; Qian, T., Lu, D. *Powder Technol.* **2006**, *161*, 185–189.

29. Neppolian, B.; Wang, Q.; Jung, H.; Choi H. *Ultrason. Sonochem.* **2008**, *15*, 649–658.

30. Akşener, E.; Figen, A. K.; Pişkin, S. *Res. Chem. Intermediat.* **2014**, *40*, 2103–2117.

31. Yılmaz, M. S.; Figen, A. K.; Pişkin, S. *Powder Technol.* **2012**, *215–216*, 166–173.

32. Derun, E. M.; Kipcak, A. S.; Senberber, F. T.; Yilmaz, M. S. *Res. Chem. Intermediat.* **2013**, doi:10.1007/s11164-013-1237-6.

33. Yongzhong, J.; Shiyang, G.; Shuping, X.; Lun, L. *Spectrochim. Acta Part A* **2000**, *56*, 1291–1297.

34. Ellsfah, E. M.; Enousi, A.; Zhang, J.; Song, H. S.; Tang, C. *Mater. Lett.* **2007**, *61*, 4358–4361.

35. Zhang, J.; Li, Z.; Zhang, B. *Mater. Chem. Phys.* **2006**, *98*, 195–197.

36. Ma, R.; Bando, Y.; Sato. T. *Appl. Phys. Lett.* **2002,** *81*, 3467–3469.

37. Fogler, H. S. *Element of Chemical Reaction Engineering,* 3rd edn, Prentice-Hall: New Jersey, USA, 1999.